Economic Geology
Vol. 97, 2002, pp. 1127–1138

THE SERRA PELADA Au-Pd-Pt DEPOSIT, CARAJÁS MINERAL PROVINCE, NORTHERN BRAZIL: RECONNAISSANCE MINERALOGY AND CHEMISTRY OF VERY HIGH GRADE PALLADIAN GOLD MINERALIZATION

A. R. Cabral, B. Lehmann,†

Institut für Mineralogie und Mineralische Rohstoffe, Technische Universität Clausthal, Adolph-Roemer-Strasse 2A, D-38678 Clausthal-Zellerfeld, Germany

R. Kwitko,

Companhia Vale do Rio Doce—CVRD, Centro de Desenvolvimento Mineral, Rodovia BR 262/ km 296, Caixa Postal 09, 33030-970 Santa Luzia-MG, Brazil

and C.H. Cravo Costa

Companhia Vale do Rio Doce—CVRD, Diretoria de Metais Nobres, Caixa Postal 51, Serra dos Carajás, 68516-000 Parauabepas-PA, Brazil

Abstract

A historic drill core from the Serra Pelada open pit was only recently assayed and has spectacular gold, palladium, and platinum grades over a 43-m-depth interval (4,709 g/t Au, 1,174 g/t Pd, 204 g/t Pt). The Au-Pd-Pt mineralization in a bonanza-grade interval (54.5–55.0 m @ 132,000 g/t Au, 11,400 g/t Pd, 359 g/t Pt) consists of coarse-grained, up to several centimeter-large, dendritic palladian gold aggregates (Au_7Pd) with abundant inclusions of guanglinite (Pd_3As), "stibio-guanglinite" ($Pd_3[As,Sb]$), sudovikovite ($PtSe_2$), palladseite ($Pd_{17}Se_{15}$), and an unnamed Pd-Pt-Se alloy. The palladian gold aggregates are often coated by goethite and are embedded in a powdery, ferruginous, clay-rich matrix with fragments of vein quartz. Iron and manganese oxides occur as vug fillings in palladian gold and are associated with native palladium and Pd-oxygenated compounds.

The near-surface bonanza palladian gold mineralization is part of a larger, deeply weathered, hydrothermal system which, in deepest drill holes (>300 m), has a relict sulfide assemblage with a variable degree of overprint by iron oxides, sericite, and kaolinite. The deep system still has gold, palladium, and platinum grades in the g/t range and displays erratically high contents in light rare earth elements, bismuth, and selenium. Drill core samples from intermediate depth (157–275 m) are high in gold, palladium, and platinum and show a very pronounced bismuth enrichment, as well as enrichment in iridium, mercury, rare earth elements, uranium, copper, and lead. The shallow drill core is extremely enriched in gold, palladium, platinum, mercury, and manganese.

The occurrence of gold dominantly as an Au-Pd alloy, the abundant selenide and arsenide inclusions in palladian gold, and the characteristic mercury signature point to an origin of the near-surface bonanza ore from a sulfur-deficient hydrothermal system, with apparently only minor supergene precious metal enrichment.

Introduction

The Serra Pelada gold deposit was discovered in 1980 by garimpeiros (artesanal miners) and was the site of the most spectacular gold rush in recent history. Within months news of bonanza gold ore attracted up to 80,000 people (Fig. 1). According to Meireles and Silva (1988), 32.6 metric tons (t) of gold were manually extracted from a 300 × 400-m pit (garimpo) which, at a depth of about 130 m, collapsed and flooded in 1984. However, it is estimated that a total of 60 to 70 t of gold was recovered from the Serra Pelada garimpo (Companhia Vale do Rio Doce—CVRD, unpublished internal information). The important grade of palladium and platinum was not realized during this period of activity. The remaining reserve of Serra Pelada is currently estimated at 3.7 Mt @ 15.20 g/t Au, 4.09 g/t Pd, and 1.89 g/t Pt (CVRD, unpublished internal information).

The Serra Pelada system is unique in terms of its size, with a total metal content of about 110 t Au, 35 t Pd, and 18 t Pt (Grainger et al., 2002), and of its anomalous Au-Pd-Pt metal association, which is poorly understood and documented in the literature (Henwood, 1871; Hussak, 1904, 1906; Guimarães, 1970; Carville et al., 1990; Stanley et al., 1990; Olivo et al., 1995; McDonald et al., 1999; Moroni et al., 2001). Recent work by Groves et al. (2001) and Grainger et al. (2002) suggests that Serra Pelada could be the most distal, low-temperature variant in the broad iron oxide copper-gold group, which is thought to comprise deposits such as Olympic Dam in South Australia (Oreskes and Einaudi, 1990), Palabora in South Africa (Groves and Vielreicher, 2001), and the Cu-Au deposits of the Carajás region (Tallarico et al., 2000a; Villas and Santos, 2001).

The gold of Serra Pelada is reported to be alloyed with palladium (Meireles and Silva, 1988); however, no study of the Serra Pelada high-grade gold ore has ever been published. The bonanza ore is now inaccessible and/or mined out, but we had the opportunity to sample a high-grade drill core from the central part of the open pit at a depth interval of 54.0 to 66.0 m (SP-32 drilled in 1982). This drill core was drilled

† Corresponding author: e-mail, lehmann@min.tu-clausthal.de

FIG. 1. The Serra Pelada garimpo in September 1983 (photo by Arthur Bernadelli); about 80,000 garimpeiros worked in extremely insalubrious conditions. The pit collapsed and flooded in 1984.

under then very crude circumstances, was assayed for gold and palladium, and stored away. Only recently, the drill core was rediscovered and re-assayed. Our short paper is not intended to be an exhaustive review of Serra Pelada nor to provide a conclusive genetic model, but it aims at providing the first mineralogical and chemical data on the exceptional bonanza mineralization which triggered the gold rush. Our study suggests that the high-grade palladian gold mineralization is probably hypogene in origin, despite the deep lateritic weathering.

Geologic Setting and Mineralization of the Serra Pelada Deposit

The Serra Pelada Au-Pd-Pt deposit is hosted in a folded, low-grade metamorphic fluvial to shallow-marine sequence of Late Archean age (Rio Fresco Formation), consisting of conglomerate, sandstone, dolomitic marble, and siltstone (Cunha et al., 1984; DOCEGEO, 1988; Meireles and Silva, 1988; Tallarico et al., 2000b; Fig. 2). The Rio Fresco Formation rests unconformably on the Archean volcano-sedimentary Rio Novo sequence. The latter is intruded by the Archean (2763 ± 6 Ma; Machado et al., 1991), chromite- and PGE-mineralized Luanga mafic-ultramafic complex, a few kilometers east-southeast from Serra Pelada (Suita and Nilson, 1988; Diella et al., 1995). Granitic magmatism in the Serra Pelada area is represented by the Cigano Granite (1883 ± 2 Ma; Machado et al., 1991), 14 km to the west. Dioritic and granodioritic rocks of unknown age were intercepted in deep drill holes during recent gold exploration of the Serra Pelada system (Tallarico et al., 2000b). A more detailed account of the geologic setting of the Carajás mineral province can be found in DOCEGEO (1988), Dardenne and Schobbenhaus (2001), Moroni et al. (2001), and Villas and Santos (2001).

The mineralization at Serra Pelada occurs in the deeply weathered hinge zone of a recumbent syncline along the contact between dolomitic marble and carbonaceous metasiltstone of the Rio Fresco Formation (Tallarico et al., 2000b). The deep-seated (>150 m in depth) mineralization is in brecciated, fine-grained, variably silicified and hematitized, carbonaceous rocks (2–10 wt % of amorphous carbon) with large amounts of kaolinite, goethite, and manganese oxide (Tallarico et al., 2000b). Stockwork-style quartz veining with

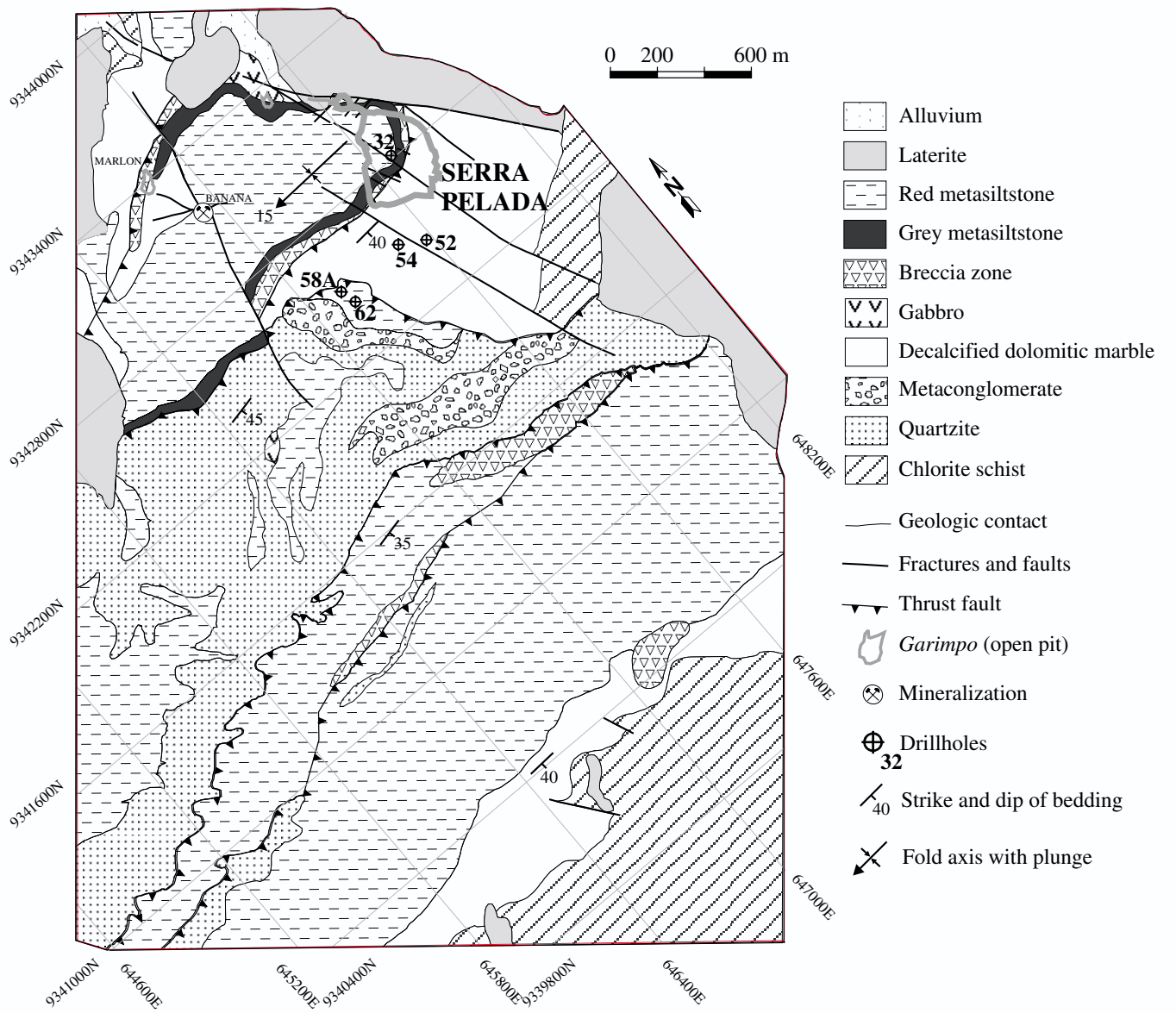

FIG. 2. Simplified geologic map of the Serra Pelada area (from Tallarico et al., 2000b) with locations of the drill holes of Tables 1 and 2. The Serra Pelada garimpo (open pit) is delineated by thick gray lines. Coordinates are in UTM.

minor sulfides, and sericite and chlorite alteration of the wall rocks predated the brecciation stage with iron oxide flooding and kaolinite formation (Tallarico, 1995). The near-surface mineralization is of the same breccia style as that found at depth but is characteristically disaggregated with coarse-grained palladian gold and fragments of hydrothermal quartz in powdery, clayey, ferruginous masses. Worthy of note is the presence of specular hematite breccia fragments in the dumps, which are, however, barren (Tables 1 and 2).

Near-Surface Bonanza Ore

Drill core SP-32 was vertically drilled in the middle of the Serra Pelada open pit during the peak of garimpo activity. The upper 40 m of the drill core consist of weathered, well-bedded red metasiltstone. The deeper drill core consists of extremely altered, soft, carbon-rich, clayey and powdery material rich in manganese and iron oxide-hydroxides. The primary textural relationships are obliterated. Small rock fragments (up to centimeters in size) of (1) white, kaolinite-rich material, (2) gray, silica-rich material, (3) black, carbon-rich phyllite, and (4) red, hematite-rich material suggest that the original rock could have been a breccia. The exceptional gold, palladium, and platinum grades over the depth interval of 40 to 87 m are plotted in Figure 3. The Au/Pd ratio varies from <1 to 100, and there is a tendency of increasing Au/Pd with depth. The Pd/Pt ratio does not correlate with the Au/Pd ratio and varies irregularly from 3 to 62.

The drill site had to be abandoned at the drilling depth of about 83 m and there is no information on deeper mineralization within the open-pit boundary. There is a very sharp

TABLE 1. Bulk-Rock Chemical Analyses: Precious Metals

Drill core, interval (m)	Sample no.	Rock type	Pd (g/t)	Pt (g/t)	Au (g/t)	Ag (ppm)	Ir (ppb)
SP-32, 54.0-54.5	2	Disaggregated, clayey material	8,040	432	70,700	21.2	<20
SP-32, 54.5-55.0	1	Disaggregated, clayey material	11,400	359	132,000	17.7	<20
SP-32, 55.0-55.5	3	Disaggregated, clayey material	456	23	3,650	<0.3	39
SP-32, 60.5-61.0	5	Disaggregated, clayey material	493	67	3,740	0.7	17
SP-32, 61.5-62.0	6	Disaggregated, clayey material	448	133	1,700	<0.3	<20
SP-32, 63.5-64.0	7	Disaggregated, clayey material	48	1.0	452	<0.3	25
SP-32, 65.5-66.0	4	Disaggregated, clayey material	333	20	2,720	0.4	18
SL-54, 157.36-157.85	8	Gray metasiltstone	90	85	122	<0.3	1,100
SL-54, 157.85-158.27	9	Gray metasiltstone	37	33	58	<0.3	590
SL-58A, 227.24-227.77	12	Disaggregated, clayey material	19	7.4	326	2.8	530
SL-62, 273.35-273.80	13	Gray metasiltstone	225	190	108	2.1	840
SL-62, 274.00-274.90	14	Gray metasiltstone	36	22	82	1.4	490
SL-52, 316.00-317.00	15	Carbonaceous metasiltstone	5.2	2.2	86	<0.3	<5
SL-54, 317.71-318.10	10	Gray metasiltstone	3.2	1.2	35	2.1	40
SL-54, 318.49-319.00	11	Gray metasiltstone	4.9	0.9	60	1.3	28
SL-52, 330.00-331.00	16	Carbonaceous metasiltstone	2.5	0.5	5.0	<0.3	<5
SL-52, 335.29-336.00	17	Carbonaceous metasiltstone	13	12	49	<0.3	16
SL-52, 336.00-336.44	18	Carbonaceous metasiltstone	5.7	4.2	24	<0.3	20
Garimpo dump	19	Specular hematite breccia	<0.01	<0.01	0.02	<0.3	<5
Garimpo dump	20	Mn oxide breccia	0.06	0.02	0.09	<0.3	<5

Samples represent quarter-splits of drill core intervals as indicated

Gold, palladium, and platinum by fire assay (gravimetric); iridium and silver by instrumental neutron activation spectrometry; all analyses by Actlabs, Ancaster, Ontario

n.a. = not analyzed

interface between the first 40 m of barren red metasiltstone and underlying bonanza-style mineralization in soft carbonaceous and powdery loose material. At the depth interval of 54.5 to 55.0 m, abundant coarse-grained gold aggregates (1–3 cm in length) occur within powdery, disaggregated, quartz-bearing clayey masses. This drill core interval has extremely high assay values of gold (132,000 g/t Au), palladium (11,400 g/t Pd), and platinum (359 g/t Pt) and was studied by ore microscopy and electron microprobe analysis.

The coarse-grained gold occurs as wire-haired bundles, partly of dark color due to goethite coating, and as single centimeter-long and thin (<1 mm) threads. It must be emphasized that the "gold nuggets" from Serra Pelada were characteristically dendritic; only one gold nugget, weighing 6.7 kg, was reported to be entirely massive (Meireles and Silva, 1988). SEM images reveal a dendritic, arborescent morphology of the coarse-grained palladian gold aggregates (Fig. 4). The arborescent form is notably similar to the palladian gold from Hope's Nose, Devon, England (Harrison and Fuller, 1987). Like that at Hope's Nose, the palladian gold does not exhibit the characteristic yellow color of pure gold in reflected light but has a whitish tint.

The coarse-grained gold from the 54.5- to 55.0-m interval has a remarkably homogeneous composition, with about 7 wt percent Pd and only sporadic traces of Cu and Ag (Table 3). Electron microprobe analyses of about forty individual crystals indicate a constant stoichiometry of Au_7Pd. Minor veinlets and tiny crystals of pure yellow gold (with traces of silver and iron) occur near the margins of, and attached to, palladian gold (Fig. 5A). Native palladium is observed as bright white porous masses and aggregates and as concentric bands on cavity walls in palladian gold (Fig. 5B). Found in goethite, it is intimately associated with a low-reflectance palladium-oxygen phase (Fig. 5B).

Inclusions in palladian gold are commonly 10 to 30 μm long. They are, in decreasing order of abundance: palladium arsenides, a Pd-Pt-Se phase, sudovikovite ($PtSe_2$), and palladseite ($Pd_{17}Se_{15}$) (Fig. 5B and C). Two palladium arsenides are distinguished: stoichiometric Pd_3As, known as guanglinite (Cabri and Laflamme, 1981, p. 159), which is a species not approved by the International Mineralogical Association; and palladium arsenide with 4.3 to 4.6 wt percent Sb at the expense of arsenic, maintaining the same Pd ratio of 3:1 found in guanglinite (Pd_3[As,Sb]) which we have termed "stibio-guanglinite."

The Pd-Pt-Se phase has about 72 to 75 wt percent Pd and 14 to 17 wt percent Pt (Table 4). Its Pt/Se ratio is about 1:2, suggesting an ideal formula of Pd_9PtSe_2. Deviations from this stoichiometry are attributed to exchange of palladium with platinum, corresponding to the general formula $(Pd,Pt)_{8+x}(Pt,Pd)Se_2$, where x varies from 0.5 to 1.7.

Palladseite and sudovikovite are generally associated with palladium arsenides, with which they have sharp contacts (Fig. 5C). Electron microprobe analyses are difficult to obtain due to the small crystal size (≤5 μm). One analysis (wt %) on palladseite gave 55.4 Pd, 36.4 Se, 5.0 Au, 2.6 Hg, 1.8 Pt, 0.8 Cu, and 0.2 Ag, amounting to 102.2 wt percent. The palladian gold matrix possibly contributed to the observed gold in this analysis. A sudovikovite crystal yielded (wt %) 52.8 Pt, 44.5 Se, and 0.1 Pd, with a sum of 97.3 wt percent. Both analyses agree with those of palladseite and sudovikovite from the type localities of Itabira (Davis et al., 1977) and Karelia (Polekhovskii et al., 1997), respectively.

Pd-rich oxygenated alteration halos are developed around Pd arsenide and Pd-Pt-Se phases where in contact with goethite. These halos are enriched in Mn and Hg, and also have traces of Cu, Fe, and Cl (up to 0.5 wt % Cl).

Besides goethite, an Mn oxide phase also fills in cavities in palladian gold. It is generally deposited inward on top of a

TABLE 2. Bulk-Rock Chemical Analyses: Major and Trace Elements (For rock types see Table 1)

Drill core, interval (m)	Sample no.	Ti (wt %)	Al (wt %)	Fe (wt %)	Mn (ppm)	Mg (wt %)	Ca (wt %)	Na (wt %)	K (wt %)	P (wt %)	S (wt %)	Be (ppm)	Sc (ppm)	V (ppm)	Cr (ppm)	Co (ppm)	Ni (ppm)
SP-32, 54.0-54.5	2	0.16	4.60	22.2	24,640	0.05	0.05	0.01	0.07	0.22	0.01	5	25.4	224	440	154	260
SP-32, 54.5-55.0	1	0.17	3.89	32.1	36,090	0.04	0.06	<0.01	0.03	0.27	0.01	5	26.0	251	260	265	270
SP-32, 55.0-55.5	3	0.14	2.83	55.2	4,039	0.02	0.04	<0.01	0.03	0.26	0.00	6	25.4	254	213	183	398
SP-32, 60.5-61.0	5	0.11	1.83	55.5	9,952	0.02	0.02	<0.01	0.07	0.09	0.01	2	15.5	225	219	352	353
SP-32, 61.5-62.0	6	0.11	2.30	47.4	9,373	0.03	0.03	0.01	0.03	0.17	0.01	3	20.4	190	271	261	231
SP-32, 63.5-64.0	7	0.03	1.90	11.2	33,935	0.07	0.07	0.01	0.07	0.18	0.01	3	8.0	106	85	342	425
SP-32, 65.5-66.0	4	0.06	1.71	22.1	37,590	0.08	0.05	0.04	0.07	0.10	0.01	2	10.0	116	60	424	303
SL-54, 157.36-157.85	8	0.21	5.18	3.2	10,130	0.18	0.07	0.09	1.02	0.18	0.02	5	45.6	139	236	416	141
SL-54, 157.85-158.27	9	0.29	5.66	1.3	248	0.25	0.04	0.10	1.78	0.07	0.02	3	26.8	143	208	20	34
SL-58A, 227.24-227.77	12	0.18	3.88	8.5	531	0.10	0.06	0.05	0.50	0.18	0.01	3	20.3	146	171	251	138
SL-62, 273.35-273.80	13	0.30	8.11	6.0	697	0.19	0.10	0.03	0.25	0.15	0.02	3	17.5	140	319	114	256
SL-62, 274.00-274.90	14	0.27	5.81	14.4	616	0.03	0.03	0.01	0.02	0.16	0.01	3	17.3	372	309	96	173
SL-52, 316.00-317.00	15	0.28	3.67	0.5	145	0.34	0.02	0.10	1.84	0.04	0.02	<1	15.4	139	116	5	35
SL-54, 317.71-318.10	10	0.37	6.69	4.1	391	4.26	0.06	0.11	2.18	0.03	0.08	2	13.1	149	102	129	450
SL-54, 318.49-319.00	11	0.41	7.52	1.8	80	5.11	0.08	0.17	2.96	0.04	0.01	2	14.6	151	128	113	433
SL-52, 330.00-331.00	16	0.27	3.44	0.5	169	0.43	0.02	0.08	1.13	0.04	0.01	1	10.8	105	72	12	62
SL-52, 335.29-336.00	17	0.14	5.23	1.3	50	0.19	0.02	0.10	1.55	0.08	0.01	1	15.2	270	136	4	18
SL-52, 336.00-336.44	18	0.20	4.08	1.0	44	0.18	0.03	0.09	1.32	0.07	0.01	1	11.1	192	117	4	13
Garimpo dump	19	0.01	0.15	59.0	154	0.01	0.03	<0.01	<0.01	0.01	0.01	<1	0.6	7	13	4	3
Garimpo dump	20	0.01	1.44	1.3	188400	0.01	0.03	0.01	0.13	0.11	0.00	3	10.4	67	<5	2650	227

Drill core, interval (m)	Sample no.	Cu (ppm)	Zn (ppm)	Ge (ppm)	As (ppm)	Se (ppm)	Rb (ppm)	Sr (ppm)	Y (ppm)	Mo (ppm)	Cd (ppm)	In (ppm)	Sn (wt %)	Sb (ppm)	Te (ppm)	Cs (ppm)	Ba (ppm)
SP-32 , 54.0-54.5	2	83	186	0.6	115	35.5	<50	61	59	<1	<0.3	1.5	<0.05	14.5	1.9	<1	2200
SP-32, 54.5-55.0	1	88	254	0.7	150	21.2	<50	96	139	<1	<0.3	1.8	<0.05	43.7	1.9	<1	3000
SP-32, 55.0-55.5	3	27	295	0.5	41.5	2.0	<50	39	123	<1	1.3	4.0	<0.05	11.9	0.8	<1	1200
SP-32, 60.5-61.0	5	40	131	0.6	27.0	0.4	<50	26	21	<1	<0.3	0.7	<0.05	9.2	0.4	<1	550
SP-32, 61.5-62.0	6	34	138	0.6	35.5	1.6	<50	32	70	<1	<0.3	1.8	<0.05	6.7	0.5	<1	410
SP-32, 63.5-64.0	7	160	215	n.a.	19.3	<3	<15	84	94	<1	<0.3	n.a.	<0.02	1.2	n.a.	<1	1900
SP-32, 65.5-66.0	4	91	139	0.2	21.0	1.2	<50	70	54	<1	0.5	1.4	<0.05	3.8	0.3	<1	1800
SL-54, 157.36-157.85	8	247	99	n.a.	22.3	<3	<15	335	84	<1	<0.3	n.a.	0.10	4.8	n.a.	8	2600
SL-54, 157.85-158.27	9	69	56	n.a.	18.5	<3	44	248	54	<1	<0.3	n.a.	0.05	0.8	n.a.	7	1400
SL-58A, 227.24-227.77	12	560	87	n.a.	36.8	<3	<15	82	64	<1	<0.3	n.a.	<0.02	0.7	n.a.	5	800
SL-62, 273.35-273.80	13	562	165	n.a.	25.1	14	<15	35	46	<1	<0.3	n.a.	<0.01	8.7	n.a.	8	1100
SL-62, 274.00-274.90	14	451	126	n.a.	69.1	8	<15	17	39	<1	<0.3	n.a.	<0.01	3.5	n.a.	5	340
SL-52, 316.00-317.00	15	16	43	n.a.	<0.5	<3	60	84	4	<1	<0.3	n.a.	<0.01	1.2	n.a.	3	570
SL-54, 317.71-318.10	10	11	152	n.a.	4.8	30	135	26	13	<1	<0.3	n.a.	<0.02	0.5	n.a.	4	600
SL-54, 318.49-319.00	11	8	95	n.a.	2.2	29	156	46	9	<1	<0.3	n.a.	0.04	0.6	n.a.	6	860
SL-52, 330.00-331.00	16	20	45	n.a.	2.1	<3	40	73	8	<1	<0.3	n.a.	<0.01	1.4	n.a.	2	420
SL-52, 335.29-336.00	17	20	32	n.a.	6.8	<3	53	127	7	<1	<0.3	n.a.	<0.01	3.1	n.a.	3	430
SL-52, 336.00-336.44	18	16	26	n.a.	7.5	<3	44	120	3	4	<0.3	n.a.	<0.01	1.4	n.a.	3	370
Garimpo dump	19	8	11	n.a.	2.5	<3	<15	3	<1	<1	0.9	n.a.	<0.01	0.6	n.a.	<1	<50
Garimpo dump	20	1338	169	n.a.	5.0	<3	<15	42	173	<1	<0.3	n.a.	<0.01	0.5	n.a.	<1	21000

TABLE 2. *(Cont.)*

Drill core, interval (m)	Sample no.	Hf (ppm)	W (ppm)	Hg ppb	Tl (ppm)	Pb (ppm)	Bi (ppm)	Th (ppm)	U (ppm)	La (ppm)	Ce (ppm)	Nd (ppm)	Sm (ppm)	Eu (ppm)	Tb (ppm)	Yb (ppm)	Lu (ppm)
SP-32, 54.0-54.5	2	4	11	334	0.5	59	8.8	10.2	16.6	31.5	87	<50	12.5	3.3	2.5	8.0	1.20
SP-32, 54.5-55.0	1	2	15	241	0.6	36	9.6	10.5	18.5	34.5	97	<51	16.8	4.6	4.0	13.8	1.99
SP-32, 55.0-55.5	3	7	18	555	<0.1	<3	4.4	10.8	13.8	31.9	63	30	14.2	1.2	3.6	14.1	2.01
SP-32, 60.5-61.0	5	2	18	1,170	<0.1	<3	4.2	8.7	20.3	32.5	40	30	5.4	1.6	1.2	3.3	0.49
SP-32, 61.5-62.0	6	3	13	49,200	<0.1	4	4.0	12.3	29.9	37.8	66	36	9.1	2.7	2.2	7.7	1.07
SP-32, 63.5-64.0	7	2	<1	5,547	n.a.	290	<2	2.0	<0.5	16.4	32	16	8.7	2.7	2.3	7.3	1.15
SP-32, 65.5-66.0	4	1	18	890	0.1	32	2.1	3.5	13.4	19.5	47	19	6.3	2.0	1.4	5.5	0.83
SL-54, 157.36-157.85	8	6	27	414	n.a.	1294	979	23.0	65.1	979	1200	240	35.8	10.0	4.9	6.4	0.96
SL-54, 157.85-158.27	9	5	<1	130	n.a.	391	293	21.0	33.2	690	803	144	15.7	3.8	1.8	3.8	0.56
SL-58A, 227.24-227.77	12	2	<1	562	n.a.	345	582	11.0	33.8	30.0	48	30	10.3	3.6	2.5	5.9	0.89
SL-62, 273.35-273.80	13	5	19	1,048	n.a.	289	205	15.7	98.8	57.3	89	30	7.0	3.2	2.9	8.9	1.38
SL-62, 274.00-274.90	14	5	16	989	n.a.	493	92	18.0	125	20.6	40	21	9.2	3.8	3.9	10.5	1.61
SL-52, 316.00-317.00	15	3	10	100	n.a.	47	2	8.4	2.6	176	276	113	16.7	2.2	<0.5	2.3	0.36
SL-54, 317.71-318.10	10	5	<1	26	n.a.	54	59	20.7	9.0	57.8	94	38	7.3	1.0	<0.5	3.6	0.54
SL-54, 318.49-319.00	11	4	<1	69	n.a.	53	36	21.1	7.3	216	238	59	6.1	1.0	<0.5	1.5	0.23
SL-52, 330.00-331.00	16	2	4	22	n.a.	29	<2	5.3	3.0	180	235	94	6.4	0.7	<0.5	1.8	0.28
SL-52, 335.29-336.00	17	4	<1	63	n.a.	47	7	12.7	11.1	506	596	135	5.9	0.6	0.6	3.4	0.52
SL-52, 336.00-336.44	18	2	<1	28	n.a.	44	<2	10.8	6.0	456	667	142	3.9	0.5	<0.5	2.0	0.31
Garimpo dump	19	<1	370	12	n.a.	<3	<2	0.6	1.8	1.8	<3	<5	0.3	<0.2	0.5	<0.2	<0.05
Garimpo dump	20	<1	<1	675	n.a.	37	<2	<0.2	12.5	31.2	63	41	18.3	6.7	5.9	23.1	3.45

Chemical analyses were carried out by Actlabs, Ancaster, Ontario; samples no. 7 to 20 were analyzed by INAA (As, Ba, Br, Ce, Co, Cr, Cs, Eu, Fe, Hf, La, Lu, Na, Nd, Rb, Sb, Sc, Se, Sm, Sn, Ta, Th, Tb, U, W, Y, and Yb); the remaining elements by ICP-OES after acid digestion; aluminum may not be totally digested; in samples no. 1 to 6 some elements (Ge, Se, In, Te, Tl, and Bi) were obtained by ICP-MS on acid digest solution; Tl may not be total; Hg was determined by cold vapor FIMS; n.a. = not analyzed

FIG. 3. Distribution of gold, palladium, and platinum with depth in drill core SP-32. Gold was determined by atomic absorption spectroscopy (aqua regia digestion) at CVRD; palladium and platinum by fire assay at Nomos, Rio de Janeiro (CVRD, internal files). The upper 40 m of the drill core consist of barren, red metasiltstone; the bonanza-style Au-PGE mineralization is hosted in soft, clayey, organic carbon-rich and powdery ferruginous material with fragments of silica-, kaolinite-, and hematite-altered carbonaceous phyllite. Seven 0.50-m drill core intervals in the 54.0- to 66.0-m-depth range were sampled and assayed (Table 1), confirming the earlier CVRD data. Drill core and data on the interval 67.5 to 71.0 m are missing.

concentric goethite band and may contain up to 0.7 wt percent Pt. The Mn content varies from 53 to 56 wt percent; qualitative EDS analysis showed subordinate peaks of P, Ba, Al, and K. Rare crystals of yttrium phosphate (xenotime or churchite) are also found attached to palladian gold in vugs. Equally rare is an acicular Al oxide phase included in palladian gold, which could be diaspore (AlO[OH]).

Deep-Seated Mineralization

Some samples from drill core below 150-m drilling depth were investigated in order to compare with the near-surface mineralization. Only a few samples were taken from several drill cores south of the open pit (Fig. 2, Table 1). This mineralization style was recently studied by Tallarico et al. (2000b) and Moroni et al. (2001).

The deeper drill cores invariably exhibit a brecciated fabric consisting of fine- to coarse-grained, angular clasts of vein quartz, altered carbonaceous rock (hematitized and chloritized), and silicified fragments in a ferruginous matrix. Relics of a primary sulfide assemblage make up a few percent of the rock and occur in the ferruginous breccia matrix and in vein

FIG. 4. Backscattered electron images of palladian gold, drill core SP-32, depth interval 54.5 to 55.0 m. A. Arborescent morphology of the wire-haired palladian gold nuggets. B. Native palladium (bright white) in iron oxy-hydroxide coatings on gold. C. Detail of palladian gold with apparent fivefold symmetry (arrows). Note occurrence of pits on the gold surface.

TABLE 3. Electron Microprobe Analyses of Coarse-Grained Palladian Gold

Column	1	2	3	4	5	6	7	8	9	10	11	12	13	14	15	16	17	18	19	20
Wt percent																				
Au	92.85	93.33	93.00	92.07	92.45	92.56	92.91	92.47	91.89	92.52	93.49	91.92	92.70	93.13	92.88	92.73	93.08	92.96	93.61	93.19
Pd	6.89	7.02	6.97	6.97	6.90	7.17	7.38	7.06	7.16	7.41	7.27	7.28	7.25	7.15	7.19	7.25	7.20	7.30	7.01	7.36
Ag	n.d.	n.d.	n.d.	n.d.	n.d.	0.20	n.d.	n.d.	0.27	n.d.	n.d.	n.d.	n.d.	0.24	0.22	0.19	0.26	0.19	n.d.	n.d.
Cu	n.d.	n.d.	n.d.	n.d.	n.d.	0.05	0.09	0.09	0.13	0.10	0.07	0.08	n.d.	n.d.	n.d.	0.12	n.d.	0.08	0.08	0.13
Total	99.74	100.35	99.97	99.04	99.35	99.98	100.38	99.62	99.45	100.03	100.83	99.28	99.95	100.52	100.29	100.29	100.54	100.53	100.70	100.68
Atomic proportions based on 8 atoms																				
Au		7.030	7.022	7.032	7.023	7.026	6.963	6.967	7.000	6.931	6.937	6.985	6.970	6.991	6.976	6.971	6.942	6.967	6.946	7.010	6.953
Pd		0.970	0.978	0.968	0.977	0.974	0.993	1.018	0.985	0.994	1.033	1.000	1.015	1.009	0.991	0.999	1.005	0.997	1.010	0.972	1.016
Ag							0.030			0.045					0.033	0.030	0.026	0.036	0.026		
Cu							0.015	0.015	0.015	0.030	0.030	0.015	0.015				0.028		0.019	0.019	0.030

Microprobe analyses were carried out at TU Clausthal using a Cameca SX100 under 20 kV and 40 nA; X-ray emission lines and standards were as follows: Au*L*a, Pd*L*a, and Ag*L*b (pure metals), and Cu*K*a ($CuFeS_2$).

Drill core SP-32, depth interval 54.5–55.0 m; n.d. = not detected

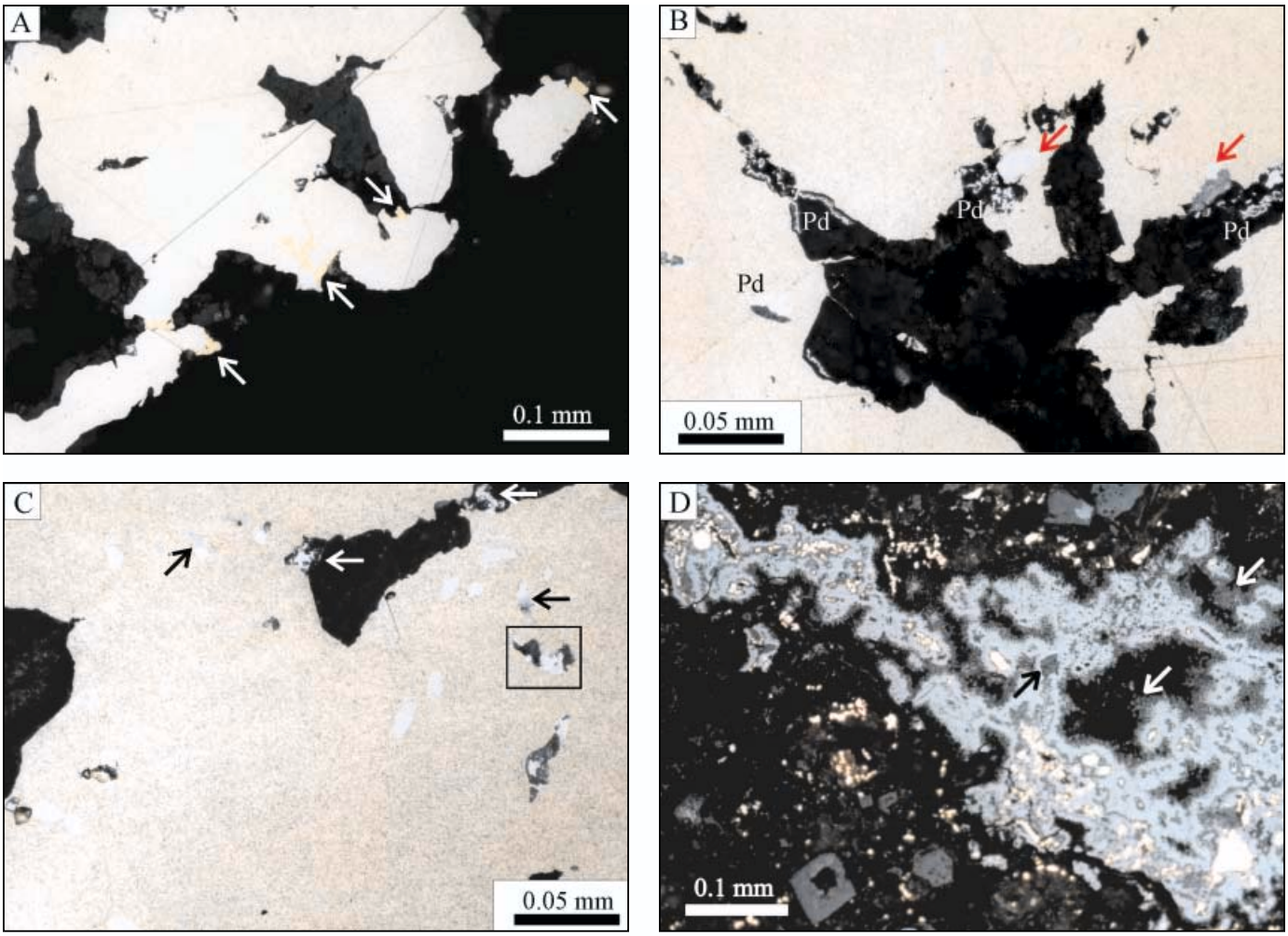

FIG. 5. Photomicrographs (reflected light, oil immersion) of coarse-grained palladian gold aggregates (A-C, drill core SP-32, depth interval 54.5–55.0 m) and ferruginous breccia (D, drill core SL-58A, 216.30 m deep). A. Palladian gold (white) with pure yellow gold crystals and veinlets (arrows). B. Cavity (dark) in palladian gold where native palladium (Pd) occurs as concentric rim (white) and reniform aggregates. Native palladium is also partially enclosed by palladian gold. The red arrows indicate an unnamed Pd-Pt-Se phase (ideally Pd_9PtSe_2), incipiently altered to a Pd-O compound. The red arrow to the far right denotes a more pronounced alteration (gray) of this Pd-Pt-Se phase. C. Palladian gold with inclusions of guanglinite and Pd and Pt selenides (black arrows). The white phase in the dark vug (white arrows) is native palladium associated with a palladium-oxygen compound and iron oxy-hydroxide. The rectangle denotes native palladium (white) and a Pd-Mn-Pb-O phase (gray) with subordinate Ba and traces of Cl. D. Mass of romanèchite (ideally $[Ba,H_2O]_2[Mn^{4+},Mn^{3+}]_5O_{10}$] (gray) with abundant gold inclusions (up to 2 wt % Ag, light yellow). Romanèchite is lined by Co-Ni-Cu-bearing lithiophorite $[(Al,Li)Mn^{4+}O_2(OH)_2]$ (white arrows) and has inclusions of Cl-bearing iron oxy-hydroxide (black arrow). The ferruginous matrix (dark) contains gold (light yellow) and Cl-bearing, goethite-like aggregates (gray), as well as Cl-bearing kaolinite crystals (not shown). This matrix cements a breccia composed predominantly of vein quartz.

quartz fragments. The primary sulfide assemblage is almost completely replaced by iron oxy-hydroxide and hematite, with a few traces of pyrite left. The ferruginous breccia matrix consists of masses of hematite, goethite, barium-rich manganese oxide, kaolinite, Ba-rich sericite, and accessory hydrous phosphates. Rutile, zircon, and apatite were observed in vein quartz. According to Tallarico et al. (2000b), the mineralogy of the deep-seated mineralization is dominated by quartz (10–60 vol %), hematite (1–40 vol %), goethite (1–15 vol %), Mn oxides (1–15 vol %), sericite (1–30 vol %), kaolinite (1–20 vol %), and amorphous carbon (1–10 vol %).

Gold occurs in manganese oxide and ferruginous aggregates in the breccia matrix (Fig. 5D). Its composition ranges from almost pure gold to gold with 2.1 wt percent Ag. Palladium is sporadically alloyed with gold, reaching up to 2.2 wt percent Pd; however, palladium is preferentially combined with mercury and forms relics of Pd-Hg alloys within porous, iron oxy-hydroxide aggregates.

The iron oxy-hydroxide aggregates form pseudomorphs of cubic and rhombic shape (Fig. 5D). Electron microprobe analyses of these phases indicate that the iron oxy-hydroxides contain bismuth (up to 2 wt %), lead (up to 1 wt % Pb), and chlorine (up to 0.6 wt % Cl). Traces of nickel, cobalt, and copper were also detected.

Within the ferruginous matrix there are euhedral, <50 μm-long laths of iron-poor kaolinite (up to 0.6 wt % Fe) with

TABLE 4. Electron Microprobe Analyses of the Pd-Pt-Se Inclusions in Coarse-Grained Palladian Gold[1]

Column	1	2	3	4	5	6	7	8	9	10
wt %										
Pt	13.80	13.89	14.82	14.87	15.54	13.89	14.95	16.88	14.56	16.50
Pd	74.10	75.13	74.40	73.95	73.44	74.46	74.06	72.34	73.81	72.53
Se	12.22	11.48	11.90	12.12	11.91	12.31	11.79	11.57	12.19	11.50
Total	100.12	100.50	101.12	100.94	100.89	100.66	100.80	100.79	100.56	100.53
Atom %										
Pt	7.70	7.70	8.21	8.22	8.69	7.92	8.35	9.52	8.13	9.31
Pd	75.49	76.57	75.49	75.22	74.92	74.69	75.49	74.40	75.19	74.70
Se	16.81	15.73	16.31	16.56	16.39	17.39	16.16	16.08	16.68	15.99
Se:Pt	2.18:1	2.04:1	1.99:1	2.02:1	1.89:1	2.20:1	1.94:1	1.69:1	2.05:1	1.72:1
Atomic proportions based on Se=2.000										
Pt	0.916	0.979	1.007	0.993	1.060	0.910	1.034	1.184	0.974	1.164
Pd	8.980	9.738	9.258	9.085	9.139	8.590	9.342	9.251	9.013	9.343

The analytical conditions are the same indicated in Table 2, with the addition of Pt ($L\alpha$) and Se ($L\alpha$); both with pure metals as standards
[1] drill core SP-32, 54.5-55.0 m

chlorine (up to 0.14 wt % Cl). Kaolinite also occurs as aggregates on fine-grained laths of Ba-bearing sericite (up to 2.2 wt % Ba).

The vein quartz clasts commonly enclose needles of rutile and may contain tiny (<5 μm) crystals of native silver and, rarely, native bismuth. Pyrite and intergrowths of pyrite and clausthalite (PbSe), as well as apatite and sericite, are also found within vein quartz.

Apart from minor pyrite, no other sulfides could be identified in the investigated samples; however, minor chalcopyrite, arsenopyrite, covellite, bornite, galena, and Ni-Co-Cu sulfides are reported by Tallarico et al. (2001b).

The ore fabric indicates that a primary quartz sulfide assemblage was brecciated and replaced by iron oxides, accompanied by hematitization and kaolinization (Tallarico, 1995). It appears that sulfide abundance is not related to precious metal enrichment (Moroni et al., 2001); gold is sited in the ferruginous breccia matrix (Tallarico, 1995).

In the deeper parts of Serra Pelada (>300-m drilling depth), fresh dolomitic marble consists of granoblastic dolomite (20–85 vol %) and minor calcite (1–15 vol %) with variable amounts of actinolite (5–50 vol %), chlorite (1–20 vol %), biotite (1–20 vol %), talc (1–10 vol %), and rare diopside. Accessory minerals are thorite, baddeleyite, titanite, allanite, tourmaline, and molybdenite (Tallarico et al., 2000b). Chloritization of actinolite, talc, and biotite is widespread and accompanied by the formation of magnetite (up to 20 vol %) and pyrrhotite in equilibrium with pyrite and chalcopyrite (Tallarico et al., 2000b).

Bulk-Rock Chemistry

Chemical data on the shallow drill core SP-32 and some additional samples from deeper drill cores up to 500 m south of the open pit are listed in Tables 1 and 2. The samples display an extreme variation range of four orders of magnitude and more for gold, palladium, platinum, mercury, and manganese, with very strong enrichment of the shallow drill core by these elements (54–66-m depth, compare Fig. 3). Drill core samples from the intermediate depth range of 157 to 275 m have high values of gold, palladium, platinum, iridium, and mercury but show a very pronounced enrichment in bismuth (1,000–10,000 times upper continental crust), as well as enrichment in light rare earth elements, uranium, copper, and lead. The deepest drill core intervals (316–336 m) still have gold, palladium, and platinum grades in the g/t range and display erratically high values in light rare earth elements, bismuth, and selenium.

It is interesting to note that only samples from the intermediate depth range are strongly enriched in iridium, not those from the near-surface bonanza Au-Pd-Pt ore zone (Table 1). Moroni et al. (2001) also identified iridium enrichment in this depth range. It appears likely that this metal zoning is a primary feature of the hydrothermal system. The very low solubility of iridium in surface waters (much lower than that of other PGE and gold) and its tendency to adsorb to ferromanganese or organic material can be expected to immobilize iridium during weathering (Anbar et al., 1996).

Both near-surface and deep-seated drill core intervals show positive correlations of Au vs. Pd, and Pd vs. Pt (Fig. 6A and B). A positive As vs. Pd trend is also apparent both for the near-surface and the deep-seated samples (Fig. 6C). In the near-surface samples, this trend is consistent with the presence of palladium arsenide inclusions in coarse-grained palladian gold; however, no palladium arsenide or As-rich minerals were identified in the deep-seated samples. There is a positive correlation between Pd and Hg for the deep-seated intervals (Fig. 6D), reflecting the occurrence of Pd-Hg alloys. The near-surface samples exhibit scatter in the distribution of Pd and Hg at the high end. Potarite (PdHg) and atheneite ($[Pd,Hg]_3As$) were documented in the near-surface intervals of drill core SP-32 (Kwitko, 1995).

The data for Hg and Mn are poorly correlated with depth, although the near-surface Mn-rich samples are richer in Hg (Fig. 6E). This may indicate that much of the near-surface mercury is fixed in manganese oxide phases. The incorporation of heavy metals into manganese oxides is also shown by the Bi + Pb vs. Mn (Fig. 6F) and Ni + Co + Cu vs. Mn plots (Fig. 6G).

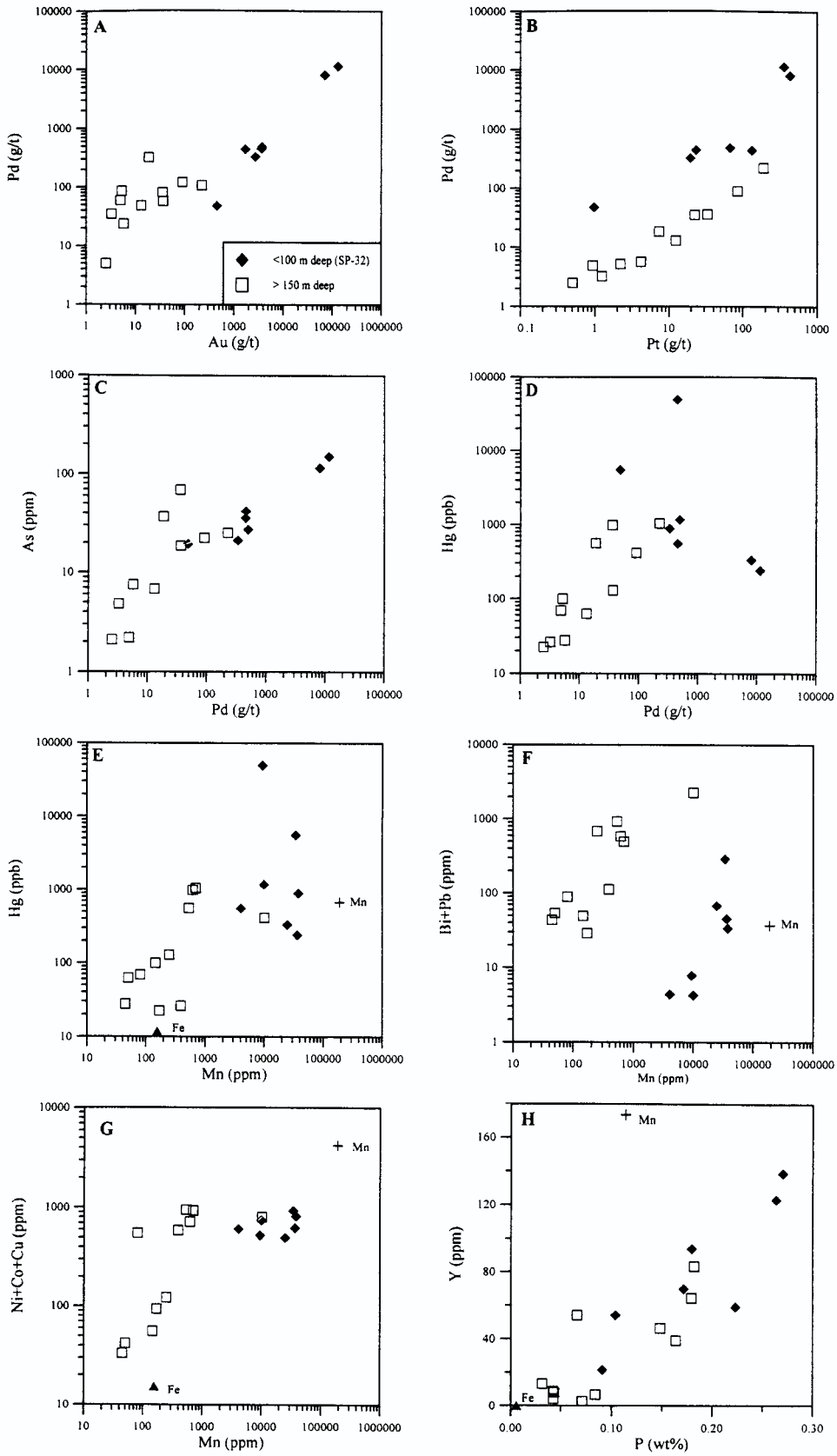

FIG. 6. Variation diagrams for some elements in drill core samples. Data are from Tables 1 and 2. Mn = Mn-rich breccia; Fe = specularite-rich breccia.

There is a positive correlation of Y vs. P which reflects the occurrence of xenotime in both the deep and near-surface environments (Fig. 6H).

Discussion

The coarse-grained and very pure palladian gold with a constant stoichiometry of Au_7Pd is unusual. We are aware of only two examples of relatively pure palladian gold recorded in the literature. These are from Sabará (8.2 wt % Pd; Seamon, 1882) and Itabira (11.6 and 19.2 wt % Pd; Hussak, 1906, and Olivo et al., 1995, respectively), both in Minas Gerais.

Supergene fluids have been invoked in metal concentration at Serra Pelada (Moroni et al., 1999, 2001; Tallarico et al., 2000b). The ore system is deeply weathered and the Carajás area has a 70-Ma-long history of lateritization (Vasconcelos et al., 1994). Chemical weathering, however, would be expected to lead to fractionation of palladium and gold rather than the formation of homogeneous palladian gold aggregates, due to the different mobility of these two metals during supergene processes (Varajão et al., 2000). The formation of pure gold, pure palladium, and palladium oxide during weathering of hydrothermal Au-Pd mineralization in the Itabira area was observed and thermodynamically explained by Olivo and Gammons (1996). We also observed micron-sized pure gold crystals and native palladium on pitted surfaces of the palladian gold aggregates and we interpret these as supergene in origin (Figs. 4 and 5A and B); however, such gold and palladium is minor compared to the abundant coarse-grained palladian gold. The palladian gold also has abundant selenide and arsenide inclusions. We are not aware of such a mineral assemblage reported for the supergene environment.

Some interesting comparisons with other Au-Pd occurrences can be drawn:

1. Coronation Hill is a low-temperature, hydrothermal Au-Pt-Pd-(Se-Sb-U) deposit in the Paleoproterozoic Pine Creek inlier of the Northern Territory, Australia (Carville et al., 1990; Mernagh et al., 1994). It was initially mined for uranium and has an indicated resource of 4.85 Mt at 4.31 g/t Au, 0.65 g/t Pd, and 0.19 g/t Pt (Carville et al., 1990). The host rock is a Lower Proterozoic volcaniclastic sequence with intrusive dioritic rocks, which are affected by pervasive sericite-chlorite alteration. The mineralization is sulfide poor and occurs in quartz-carbonate-hematite veinlets and as disseminations. Two types of mineralization have been observed: a gold-PGM-selenide association with native gold (± silver-bearing), clausthalite (PbSe), and stibiopalladinite (Pd_5Sb_2); and a gold-PGM-selenide-sulfide association with the above mineral phases plus replacive pyrite in altered igneous rocks. Fluid and mineralogic data indicate that the ore-bearing fluid was a highly oxidizing, acidic, and calcium-rich brine at around 140°C.

2. The Waterberg district in the central Bushveld, South Africa, hosts brecciated PGE-Au-bearing quartz veins in the Proterozoic metavolcanic rocks of the Rooiberg Group, which were among the first PGE ores to be exploited in South Africa (Wagner, 1929). The mineral assemblage consists of brecciated comb quartz and specularite in a vuggy matrix of iron oxy-hydroxides (with traces of primary pyrite), kaolinite, chlorite, and pyrolusite. Platinum occurs intergrown with specularite and monazite, and in the ferruginous matrix and is often alloyed with palladium (up to 45 wt % Pd). Field relations, gangue mineralogy, and fluid inclusions indicate fluid temperatures of 200° to 300°C, low salinity, and a low-pressure environment (McDonald et al., 1999).

3. Arborescent, centimeter-long palladian gold, Pd stibioarsenides, and selenide minerals, including chrisstanleyite ($Ag_2Pd_3Se_4$), are found in carbonate veins cutting hematitized limestone wall rock at Hope's Nose, Devon, England (Clark and Criddle, 1982; Harrison and Fuller, 1987; Stanley et al., 1990; Paar et al., 1998). The homogenization temperatures of fluid inclusions in calcite and quartz gangue are between 65° and 120°C, and salinities are around 20 wt percent NaCl equiv (Scrivener et al., 1982).

4. Palladian gold mineralization (jacutinga) is associated with specularite-rich veins in iron ore deposits of the Quadrilátero Ferrífero (Henwood, 1871; Hussak, 1904; Olivo et al., 1995; Varajão et al., 2000; Cabral et al., 2001). The mineralization also contains platinum and palladium selenides such as palladseite (Davis et al., 1977) and sudovikovite. The latter occurs as inclusions both in hongshiite (PtCu) (Kwitko et al., 2002) and specularite (Cabral et al., 2002). Fluid inclusion homogenization temperatures in specularite from Gongo Soco cluster at about 160°C and have around 10 wt percent NaCl equiv (V. Lüders, unpublished data).

These deposits have many features in common with Serra Pelada, and the presence of the element association of Au-Hg-As-Sb-Se-Cu correlates with the epithermal gold selenide category of Lindgren (1928). The characteristic bismuth content in deeper parts of the system and the skarn assemblage in the sedimentary host rock associated with dioritic intrusive units could point to magmatic input (Tallarico et al., 2000b). Dardenne and Schobbenhaus (2001), however, indicate that the mineralization may be related to regional shear zones which affected the dioritic intrusions (see also references therein). Our current knowledge on the Serra Pelada deposit allows no conclusive genetic model, but mineralogical and chemical evidence suggests a (low-temperature) hydrothermal origin for the coarse-grained palladian gold in the near-surface bonanza mineralization.

Acknowledgments

This contribution is part of a Ph.D. project (A.R.C.) financed by a Deutscher Akademischer Austauschdienst (DAAD) scholarship and Deutsche Forschungsgemeinschaft (DFG). We gratefully acknowledge the help of Companhia Vale do Rio Doce (CVRD), particularly, Paulo R. Amorim dos Santos Lima (Paulão), for providing access to the garimpo area and to the drill cores, polished sections, and private reports. A.R.C. is particularly grateful to Klaus Herrmann (TU Clausthal) for meticulous assistance in the electron microprobe analyses, as well as to Eike Gierth (TU Clausthal) for taking photomicrographs. The manuscript was improved by the critical readings of Gema Olivo, Marilene Moroni, and the editorial office of *Economic Geology*.

October 17, 2001; February 20, 2002

REFERENCES

Anbar, A.D., Wasserburg, H.J., Papanastassiou, D.A., and Andersson, P.S., 1996, Iridium in natural waters: Science, v. 273, p. 1524–1528.

Cabri, L.J., and Laflamme, J.H.G., 1981, Analyses of minerals containing platinum-group elements, *in* Cabri, L.J., ed., Platinum-group elements: Mineralogy, geology, recovery: CIM special volume 23, p. 151–173.

Cabral, A.R., Lehmann, B., Kwitko, R., Jones, R.D., Pires, F.R.M., Rocha Filho, O.G., and Innocentini, M.D., 2001, Palladium-oxygenated compounds of the Gongo Soco mine, Quadrilátero Ferrífero, central Minas Gerais, Brazil: Mineralogical Magazine, v. 65, p. 169–179.

Cabral, A.R., Lehmann, B., Kwitko, R., Galbiatti, H.F., and Pereira, M.C., 2002, Palladseite and its oxidation: evidence from gold-palladian vein-type mineralization (jacutinga), Cauê iron-ore mine, Quadrilátero Ferrífero, Minas Gerais, Brazil: Mineralogical Magazine, v. 66, p. 327–336.

Carville, D.P., Leckie, J.F., Moorhead, C.F., Rayner, J.G., and Durbin, A.A., 1990, Coronation Hill gold-platinum-palladium deposit: Austalasian Institute of Mining and Metallurgy Mon. 15, p. 759–762.

Clark, A.M., and Criddle, A.J., 1982, Palladium minerals from Hope's Nose, Torquay, Devon: Mineralogical Magazine, v. 46, p. 371–377.

Cunha, B.C.C., Santos, D.B., and Prado, P., 1984, Contribuição ao estudo da estratigrafia da região de Gradaús, com ênfase no Grupo Rio Fresco, *in* Congresso Brasileiro de Geologia, 33, Rio de Janeiro, Anais, Sociedade Brasileira de Geologia, v. 2, p. 873–885.

Dardenne, M.A., and Schobbenhaus, C., 2001, Metalogênese do Brasil: Brasília, Editora Universidade de Brasília, 392 p.

Davis, R.J., Clark, A.M., and Criddle, A.J., 1977, Palladseite, a new mineral from Itabira, Minas Gerais, Brazil: Mineralogical Magazine, v. 41., p. 123.

Diella, V., Ferrario, A., and Girardi, V.A.V., 1995, PGE and PGM in the Luanga mafic-ultramafic intrusion in Serra dos Carajás (Pará State, Brazil): Ore Geology Review, v. 9, p. 445–453.

DOCEGEO, Equipe-Distrito Amazônia, 1988, Revisão litoestratigráfica da Província Mineral de Carajás, *in* Província Mineral de Carajás – Litoestratigrafia e principais depósitos minerais: Congresso Brasileiro de Geologia, 35, Belém, Anexo, Sociedade Brasileira de Geologia, p. 11–56.

Grainger, C.J., Groves, D.I., and Costa, C.H.C., 2002, The epigenetic sediment-hosted Serra Pelada Au-PGE deposit and its potential genetic association with Fe-oxide Cu-Au mineralization within the Carajás mineral province, Amazon craton, Brazil: Society of Economic Geologists Special Publication 9, p. 47–64.

Groves, D.I., and Vielreicher, N.M., 2001, The Phalaborwa (Palabora) carbonatite-hosted magnetite-copper sulfide deposit, South Africa: An end-member of the iron-oxide copper-gold-rare earth element deposit group?: Mineralium Deposita, v. 36, p. 189–194.

Groves, D.I., Grainger, C.J., and Vielreicher, N., 2001, Palabora Cu and Serra Pelada Au-PGE: End members of the Fe-oxide Cu-Au deposit group [abs.]: Geological Society of America, Program with Abstracts, v. , p. A2.

Guimarães, D., 1970, Arqueogênese do ouro na região central de Minas Gerais: Departamento Nacional da Produção Mineral, Divisão de Fomento da Produção Mineral, Boletim 139, 51 p.

Harrison, S., and Fuller, J., 1987, Gold from Hope's Nose, Torquay, Devon, England: Mineralogical Record, v. 18, p. 85–88.

Henwood, W.J., 1871, On the gold mines of Minas Geraes, Brazil: Cornwall Royal Geological Society Transactions, v. 8, p. 168–370.

Hussak, E., 1904, Über das Vorkommen von Palladium und Platin in Brasilien: Kaiserlichen Akademie der Wissenschaften, Mathematisch-naturwissenschaftlichen Klasse, Sitzungsberichte, v. 113, p. 379–468.

——1906, Über das Vorkommen von Palladium und Platin in Brasilien: Zeitschrift für praktische Geologie, v. 14, p. 285–293.

Kwitko, R., 1995, Projeto Redenção: Estudos petrográficos – Relatório de progresso, Agosto 1995: Belo Horizonte, Brazil, Companhia Vale do Rio Doce, unpublished report, 24 p.

Kwitko, R., Cabral, A.R., Lehmann, B., Laflamme, J.H.G., Cabri, L.J., Criddle, A.J., and Galbiatti, H.F., 2002, Hongshiite (PtCu) from itabirite-hosted Au-Pd-Pt mineralization (jacutinga), Itabira district, Minas Gerais, Brazil: Canadian Mineralogist, v. 40, p. 711–723.

Lindgren, W., 1928, Mineral deposits, 3rd ed.: New York, McGraw Hill, 1049 p.

Machado, N., Lindenmayer, Z., Krogh, T.E., and Lindenmayer, D., 1991, U-Pb geochronology of Archean magmatism and basement reactivation in the Carajás area, Amazon Shield, Brazil: Precambrian Research, v. 49, p. 329–354.

McDonald, I., Ohnenstetter, D., Rowe, J.P., Tredoux, M., Pattrick, R.A.D., and Vaughan, D.J., 1999, Platinum precipitation in the Waterberg deposit, Naboomspruit, South Africa: South African Journal of Geology, v. 102, p. 184–191.

Meireles, E.M., and Silva, A.R.B., 1988, Depósito de ouro de Serra Pelada, Marabá, Pará, *in* Schobbenhaus, C., and Coelho, C.E.S., eds., Principais depósitos minerais do Brasil – volume III: Brasília, Departamento Nacional da Produção Mineral, Companhia Vale do Rio Doce, p. 547–557.

Mernagh, T.P., Heinrich, C.A., Leckie, J.F., Carville, D.P., Gilbert, D.J., Valenta, R.K., and Wyborn, L.A.O., 1994, Chemistry of low-temperature hydrothermal gold, platinum, and palladium (± uranium) mineralization at Coronation Hill, Northern Territory, Australia: Economic Geology, v. 89, p. 1053–1073.

Moroni, M., Ferrario, A., and Girardi, V.A.V., 1999, Towards a model for the Serra Pelada Au-Pd-Pt deposit, Serra dos Carajás, Brazil, *in* Stanley, C.J., et al., eds., Mineral deposits: Processes to processing: Rotterdam, Balkema, p. 759–762.

Moroni, M., Girardi, V.A.V., and Ferrario, A., 2001, The Serra Pelada Au-PGE deposit, Serra dos Carajás (Pará State, Brazil): Geological and geochemical indications for a composite mineralizing process: Mineralium Deposita, v. 36, p. 768–785.

Olivo, G.R., and Gammons, C., 1996, Thermodynamic and textural evidence for at least two stages of Au-Pd mineralization at the Cauê iron mine, Itabira district, Brazil: Canadian Mineralogist, v. 34, p. 547–557.

Olivo, G.R., Gauthier, M., Bardoux, M., Sá, E.L., Fonseca, J.T.F., and Carbonari, F., 1995, Palladium-bearing gold deposit hosted by Proterozoic Lake Superior-type iron-formation at the Cauê iron mine, Itabira district, southern São Francisco craton, Brazil: Geologic and structural controls: Economic Geology, v. 90, p. 118–134.

Oreskes, N., and Einaudi, M.T., 1990, Origin of rare earth element-enriched hematite breccias at the Olympic Dam Cu-U-Au-Ag deposit, Roxby Downs, South Australia: Economic Geology, v. 85, p. 1–28.

Paar, W.H., Roberts, A.C., Criddle, A.J., and Topa, D., 1998, A new mineral, chrisstanleyite, $Ag_2Pd_3Se_4$, from Hope's Nose, Torquay, Devon, England: Mineralogical Magazine, v. 62, p. 257–264.

Polekhovskii, Yu.S., Tarasova, I.P., Nesterov, A.R., Pakhomovskii, Ya.A., and Bakhcharaitsev, A.Yu., 1997, Sudovikovite $PtSe_2$—a new platinum selenide from south Karelia metasomatites: Doklady Akademia Nauk, v. 354, p. 82–85. (in Russian)

Scrivener, R.C., Cooper, B.V., George, M.C., and Shepherd, T.J., 1982, Gold-bearing carbonate veins in the Middle Devonian limestone of Hope's Nose, Torquay: Ussher Society Proceedings, v. 5, p. 393.

Seamon, W.H., 1882, Analysis of native palladium-gold from Taquaril, near Sabará, Province of Minas Geraes, Brazil: Chemical News, v. 46, p. 216.

Stanley, C.J., Criddle, A.J., and Lloyd, D., 1990, Precious and base metal selenide mineralization at Hope's Nose, Torquay, Devon: Mineralogical Magazine, v. 54, p. 485–493.

Suita, M.T.F., and Nilson, A.A., 1988, Geologia do complexo máfico-ultramáfico Luanga (Província de Carajás, Pará) e das unidades encaixantes: Congresso Brasileiro de Geologia, 35, Belém, Anais, Sociedade Brasileira de Geologia, p. 2813–2823.

Tallarico, F.H.B., 1995, Projeto Ouro-Serra Pelada: Relatório final de estudos petrográficos, Abril 1995: Belo Horizonte, Brazil, Companhia Vale do Rio Doce, unpublished report, 35 p.

Tallarico, F.H.B., de Oliveira, C.G., and Figueiredo, B.R., 2000a, The Igarapé Bahia Cu-Au mineralization, Carajás province: Revista Brasileira de Geociências, v. 30, p. 230-233.

Tallarico, F.H.B., Coimbra, C.R., and Cravo Costa, C.H., 2000b, The Serra Leste sediment-hosted Au-(Pd-Pt) mineralization, Carajás province: Brasileira de Geociências Revista, v. 30, p. 226–229.

Varajão, C.A.C., Colin, F., Vieillard, P., Melfi, A.J., and Nahon, D., 2000, Early weathering of palladium gold under lateritic conditions, Maquiné mine, Minas Gerais, Brazil: Applied Geochemistry, v. 15, p. 245–263.

Vasconcelos, P.M., Renne, P.R., Brimhall, G.H, and Becker, T.A., 1994, Direct dating of weathering phenomena by $^{40}Ar/^{39}Ar$ and K-Ar analysis of supergene K-Mn oxides: Geochimica et Cosmochimica Acta, v. 58, p. 1635–1665.

Villas, R.N., and Santos, M.D., 2001, Gold deposits of the Carajás mineral province: deposit types and metallogenesis: Mineralium Deposita, v. 36, p. 300-331.

Wagner, P.A., 1929, The platinum deposits and mines of South Africa: Edinburgh, Oliver and Boyd, 326 p.